

# V.N.20 Investigation of the Nature of Active Sites on Heteroatom-Containing Carbon Nano-Structures for Oxygen Reduction Reaction

Principal Investigator: Umit S. Ozkan

College of Engineering Distinguished Professor  
Department of Chemical and Biomolecular Engineering  
The Ohio State University  
Phone: (614) 292-6623  
Email: Ozkan.1@osu.edu

Post-doctoral Researchers:

- Xiaoguang Bao, Department of Chemistry, The Ohio State University
- Juan Tian, Burcu Mirkelamoglu and Bing Tan, Department of Chemical and Biomolecular Engineering, The Ohio State University

PhD Students:

Elizabeth J. Biddinger, Dieter von Deak, Deepika Singh, **Kuldeep Mamtani**, Department of Chemical and Biomolecular Engineering, The Ohio State University

Undergraduate Students:

Douglas S. Knapke, Katie Luthman, Jesaiah King, Dan Valco, Sai Uppati, Department of Chemical and Biomolecular Engineering, The Ohio State University

Collaborators:

- Aravind Asthagiri, Associate Professor, Department of Chemical and Biomolecular Engineering, The Ohio State University
- Christopher Hadad, Professor, Department of Chemistry, The Ohio State University
- Dr. Jeffrey Miller, Argonne National Laboratory
- Dr. Jean-Marc Millet, CNRS Catalysis Research Institute Lyon-France

DOE Program Manager: Raul Miranda

USDOE, Office of Basic Energy Sciences,  
Catalysis Science Program  
Phone: 301-903-8014  
Email: raul.miranda@science.doe.gov

nitrogen-containing carbon structures, with or without a metal center, show potential as possible replacements for Pt. What is lacking, however, is an understanding of the nature of the active sites in these materials.

## Abstract

Nitrogen-containing carbon nanostructures (CN<sub>x</sub>) have been synthesized and developed as cathode catalysts for proton exchange membrane (PEM) fuel cells in our research group at Ohio State as part of our previous work. In the last year, we have examined the growth process of CN<sub>x</sub> catalysts on two different Co-doped substrates: Vulcan carbon and Magnesia, during the decomposition of acetonitrile using *in-situ* techniques such as X-ray absorption near edges spectroscopy (XANES), extended X-ray absorption fine structure spectroscopy (EXAFS), X-ray diffraction (XRD) and *ex-situ* techniques such as X-ray photon spectroscopy (XPS), and transmission electron microscopy (TEM). The structure of CN<sub>x</sub> obtained as well as the nitrogen content was significantly different on the two substrates, which led to differences in activity, as shown by rotating ring disk electrode (RRDE). We have also recently begun synthesizing Fe-N-C catalysts, which are commonly known to be the most active non-precious metal catalysts for the oxygen reduction reaction (ORR). The active sites for Fe-N-C catalysts are thought to be Fe-N<sub>2</sub> and/or Fe-N<sub>4</sub> centers, which are possibly different from the active sites of CN<sub>x</sub> catalysts which are most likely pyridinic nitrogen groups located on graphitic edge planes. We have compared CN<sub>x</sub> and Fe-N-C catalysts in half cell and single cell tests along with the characterization techniques listed above, to elucidate the differences in the structure and active sites between the two types of catalysts.

## Progress Report

### 1. In-situ characterization of the growth of CN<sub>x</sub> carbon nano-structures as oxygen reduction reaction catalysts

*In-situ* XANES and EXAFS techniques were used to characterize the CN<sub>x</sub> growth process over two substrates (Vulcan carbon and MgO) doped with Co. Changes taking place in the growth catalyst were examined during the heat treatment and decomposition of acetonitrile over the substrates. *In-situ* XANES provided information about the ease of reduction and coordination environment of Co over Co-VC and Co-MgO substrates. Linear combination (LC) fitting analysis was performed for the spectra obtained for the two substrates at room temperature, at 800°C, after 30 min and after 2 h of acetonitrile flow with cobalt acetate, CoO, Co foil as reference compounds.

## Objectives

To investigate the nature of the active sites in CN<sub>x</sub> and Fe-N-C catalysts for the oxygen reduction reaction in proton exchange membrane (PEM) fuel cells

## Technical Barriers

In PEM and direct methanol fuel cells, the oxygen reduction reaction at the cathode leads to the major overpotential and as a result major power loss. Pt catalysts, which are the state-of-the art cathode electro-catalysts, suffer from prohibitively high cost, making the wide-spread application of fuel cells difficult. Among the alternatives,

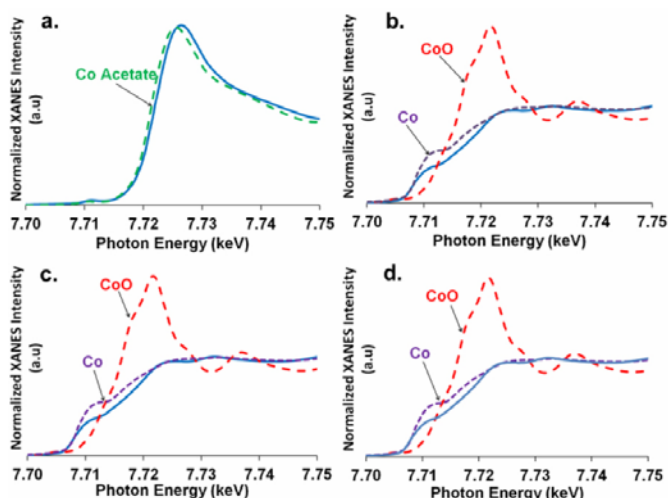


**FIGURE 1.** Normalized *in-situ* XANES spectra of Co K-edge taken during the growth of  $\text{CN}_x$  over Co-Vulcan Carbon growth substrate at different stages of pyrolysis a) room temperature, b) after treatment in  $\text{N}_2$  at  $800^\circ\text{C}$ , c) after 30 min of  $\text{CH}_3\text{CN}$  pyrolysis, d) after 2 h of  $\text{CH}_3\text{CN}$  pyrolysis (Spectra for Co acetate, CoO and Co are shown as reference).

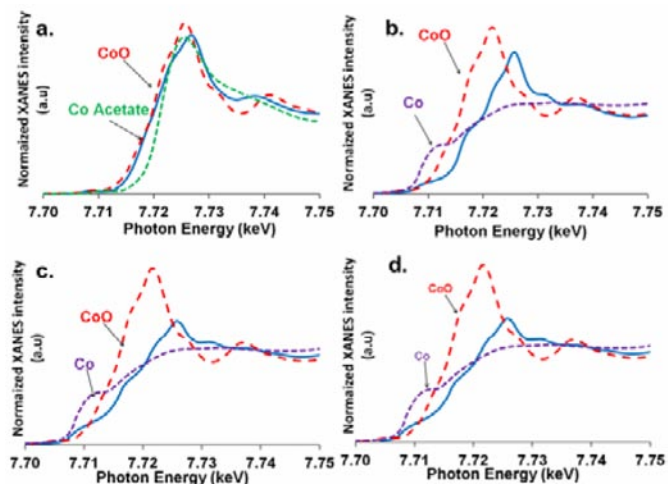


**FIGURE 2.** Normalized *in-situ* XANES spectra of Co K-edge taken during the growth of  $\text{CN}_x$  over Co-MgO substrate at different stages of pyrolysis a) room temperature, b) after treatment in  $\text{N}_2$  at  $800^\circ\text{C}$ , c) after 30 min of  $\text{CH}_3\text{CN}$  pyrolysis, d) after 2 h of  $\text{CH}_3\text{CN}$  pyrolysis.

From LC-XANES analysis of the Co-VC spectra at room temperature, cobalt species were seen to exist as cobalt acetate prior to any heat treatment (Figure 1a). Under nitrogen at  $800^\circ\text{C}$ , the sample was reduced to a mostly metallic form and remained in this state even after introduction of acetonitrile for 30 min and 2 h (Figure 1b-d). The LC-XANES fits for the Co-MgO samples showed more oxidized states for cobalt (Figure 2a), which could be explained by the presence of the oxide support. At room temperature, Co in Co-MgO exists in  $\text{Co}^{2+}$  form. Up to 40% reduction was observed under nitrogen (Fig. 2b). Metallic

cobalt became more evident upon introduction of acetonitrile for 30 min, and persisted with the same percentage contribution after 2h of acetonitrile treatment (Fig 2c and d). Co over MgO appeared to be less reduced at the end of acetonitrile treatment than over VC substrate. XANES spectra collected ex-situ for  $\text{CN}_x$  samples after acid washing was identical for both  $\text{CN}_x$  formed over MgO and Vulcan carbon (Figure 3), with over 90% metallic Co, demonstrating that although the type and abundance of cobalt phases that exist at the end of the acetonitrile pyrolysis may be different over the two growth substrates, once washed away in acid the cobalt phase left behind in  $\text{CN}_x$  is the same regardless of the substrate used.

The extended X-ray absorption fine structure (EXAFS) spectroscopy technique provides information about the coordination environment of the samples. The magnitudes of the  $k^2$  weighted Fourier Transform of the Co K-edge EXAFS spectra for Co-VC samples are shown in Figure 4a. At room temperature, the peak at the uncorrected R-value of  $1.59 \text{ \AA}$  can be attributed to the Co-O peak present in Co-acetate. After nitrogen treatment at  $800^\circ\text{C}$ , the Co-O peak disappeared with a concurrent appearance of the Co-Co peak at  $2.1 \text{ \AA}$  in the uncorrected FT-magnitude. This Co-Co peak persisted in both of the spectra taken 30 min and 2h after acetonitrile introduction. EXAFS fits were carried out using the same experimental standards used in XANES fits. After heat treatment in  $\text{N}_2$  only, and even after acetonitrile introduction for 30 mins, the cobalt particle size under *in-situ* conditions was very similar to that of bulk metallic cobalt, as indicated by the calculated coordination number (CN) values of 11.2 and 10.9 respectively.

Figure 4b shows the FT-magnitudes acquired over the Co-MgO substrate at four different stages during pyrolysis. At room temperature, there exists a peak at  $1.59 \text{ \AA}$ , which could correspond to the Co-O bond in CoO. At  $800^\circ\text{C}$  in nitrogen, a smaller peak appeared at  $1.4 \text{ \AA}$  along with a peak at  $2.6 \text{ \AA}$ , which could be due to the Co-O and Co-O-Co interactions, respectively. After reduction under acetonitrile atmosphere, the intensity of the peak at  $1.59 \text{ \AA}$  decreased, with the simultaneous occurrence of a broad peak at  $2.27 \text{ \AA}$  (uncorrected), which could be due to conjunction of Co-Co with the Co-O-Co bond contributions. EXAFS fits carried out for the samples to provide further verification that the ratios of cobalt acetate, cobalt oxide, and metallic cobalt obtained for the different sample compositions were accurate.

Transmission electron microscopy imaging helped characterize the growth of acid-washed carbon nanostructures formed upon acetonitrile pyrolysis over Co-VC and Co-MgO substrates. As seen in Figure 5a-d, after acid washing, the carbon nanostructures grown over Co-VC are in the form of stacked cups, but with less order as compared to the  $\text{CN}_x$  grown on Co-MgO (Figure 5e-h). Carbon nanostructures are less abundant in the  $\text{CN}_x$  grown over the VC support due to the majority of growth medium

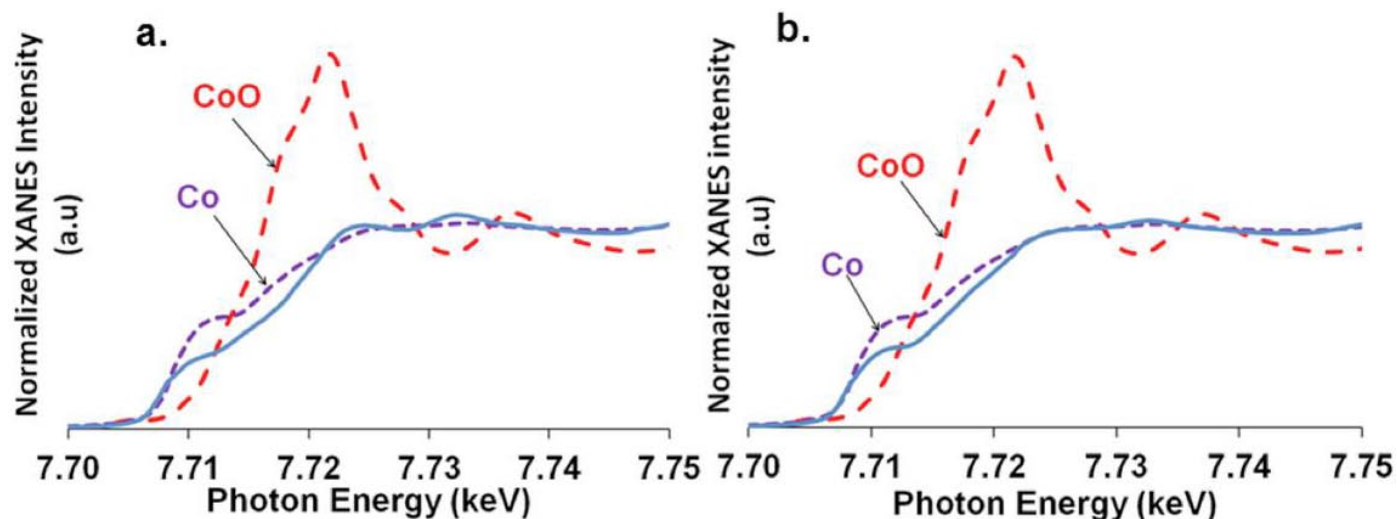


FIGURE 3. Normalized ex-situ XANES Co K-edge spectra of acid-washed CN<sub>x</sub> grown on a) Co-VC and b) Co-MgO

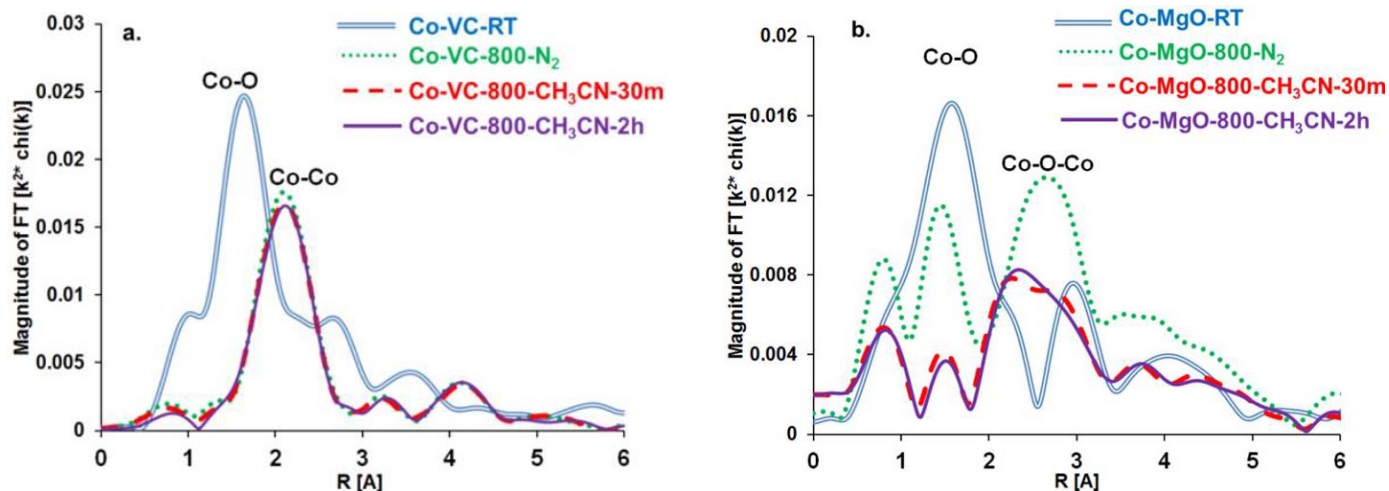


FIGURE 4. Magnitudes of  $k^2$ -weighted Fourier transforms of *in-situ* cobalt K-edge EXAFS spectra of (a) Co-VC and (b) Co-MgO growth substrates during different stages of pyrolysis

(i.e., Vulcan carbon) remaining after acid washing. The fibers are thick-walled (wall thickness~10nm), with relatively large cobalt particles encased within the carbon shell, with a diameter of approximately 25nm (Fig. 16c-d).

CN<sub>x</sub> nano-structures grown over the Co-MgO, on the other hand, are more-ordered and better-defined stacked cups, as shown in Fig. 5e, f, and g. They are more abundant because the oxide support is washed away with acid leaching, leaving only the carbon nanostructures behind. Cobalt also appeared to be encased within the nanostructures, and the particle size and wall thickness were smaller than those seen in CN<sub>x</sub> grown over Co-VC, as is the diameter of the stacked cups (Fig. 5d and h).

Electrochemical activity tests for washed and unwashed CN<sub>x</sub> grown over Co-VC and Co-magnesia were performed using RRDE technique in acidic medium. Figure 6a shows the polarization curves for the washed and unwashed samples grown over the two different growth substrates. When washed samples were compared, the CN<sub>x</sub> catalysts grown over Co-MgO were seen to be more active towards ORR than CN<sub>x</sub> grown over Co-VC. There was a difference of 50 mV between the onset potentials (Figure 6. Inset) observed over these two washed catalysts.

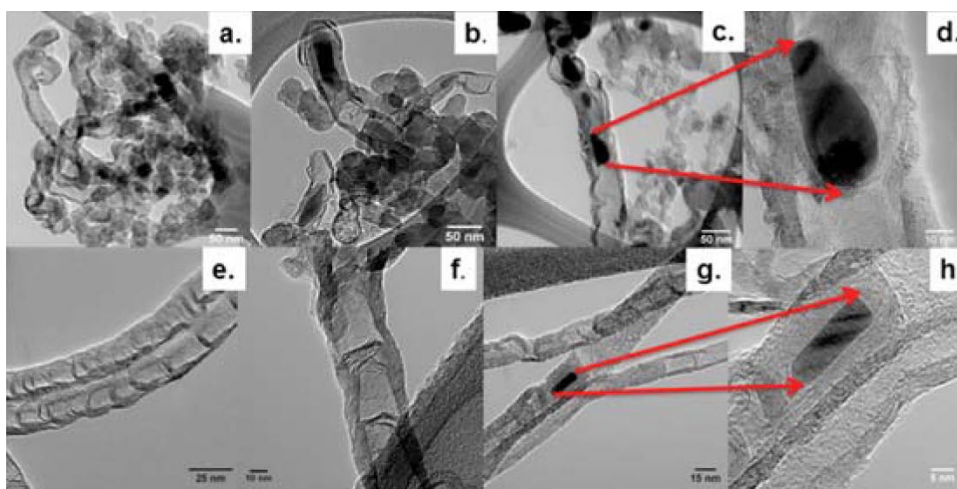


FIGURE 5. TEM images of acid-washed  $\text{CN}_x$ , grown on Co-Vulcan Carbon (a-d) and CO-MgO (e-h)

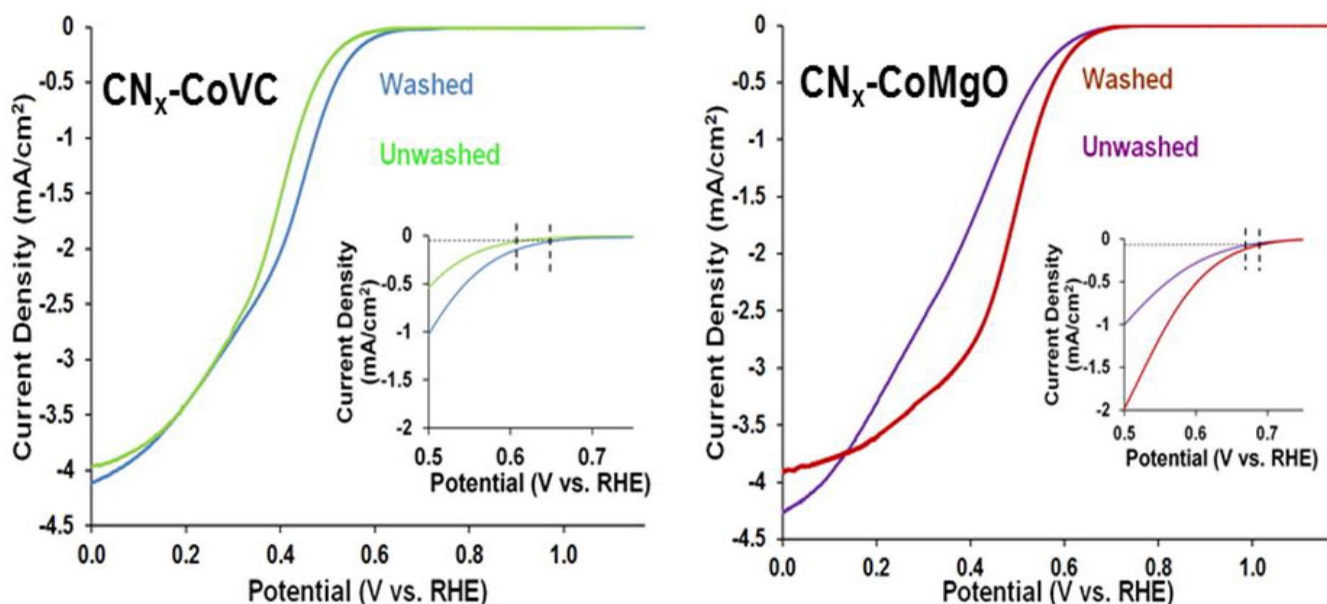


FIGURE 6. Rotating ring disk electrode (RRDE) tests of washed and unwashed  $\text{CN}_x$  catalysts grown on Co-Vulcan Carbon and Co-MgO in  $\text{O}_2$ -saturated 0.5M  $\text{H}_2\text{SO}_4$  at 25°C; rotation rate: 2500 rpm; scan rate 10 mV/s; scan direction: cathodic; catalyst loading 1.6  $\text{mg}/\text{cm}^2$ ; disk geometric area: 0.2472  $\text{cm}^2$

## 2. Investigation of differences between $\text{CN}_x$ and iron-nitrogen-carbon (Fe-N-C) catalysts for ORR

More recently reported non-precious metal ORR catalysts consist of a high surface area carbon support impregnated with 1% Fe and a nitrogen containing pore filler, heat treated in an inert atmosphere of Ar, followed by a second heat treatment in pure  $\text{NH}_3$ . The active sites in these catalysts are thought to be iron coordinated by two and/or four nitrogen atoms in a carbon matrix.

In our previous work, we have shown high ORR activity for nitrogen-doped carbon nanostructures ( $\text{CN}_x$ ) synthesized

by heat treatment of an oxide or carbon support impregnated with Fe or Co in acetonitrile. These carbon nano-structures were washed by an acid to leach out any exposed metal and non-conductive oxides. These catalysts had high pyridinic nitrogen content with significant graphitic edge plane exposure both of which correlated with ORR activity.

In an ongoing study, we are attempting to elucidate differences between Fe-N-C and  $\text{CN}_x$  catalysts. Fuel cell activity tests performed on  $\text{CN}_x$  (grown on a Fe-doped supports by acetonitrile pyrolysis) and Fe-N-C (heat treated in Ar followed by  $\text{NH}_3$ ) catalysts demonstrated that Fe-N-C catalysts were more active for ORR (Figure 7). However,

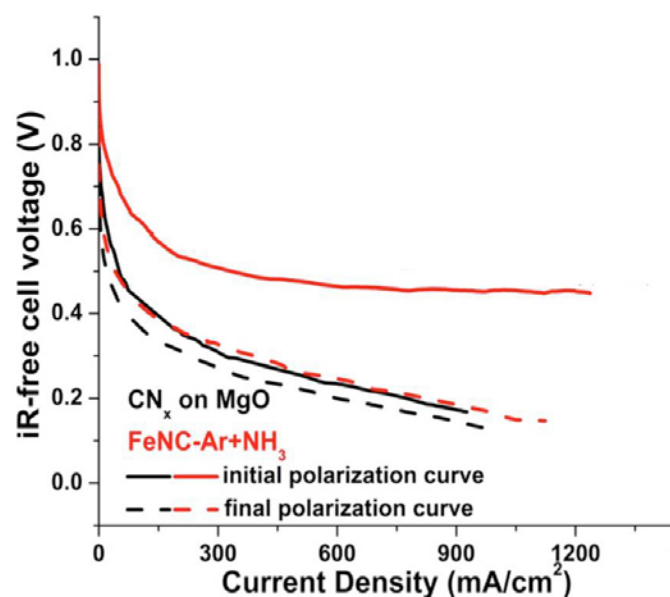


**FIGURE 7.** Fuel cell activity comparison for CN<sub>x</sub> and Fe-N-C before and after a 100-hour potential hold. Cell temperature: 80°C; Relative humidity: 100%; Backpressure: 15psig; Cathode catalyst loading 1mg/cm<sup>2</sup>; Anode catalyst: 0.5 mg Pt/cm<sup>2</sup>

fuel cell stability tests performed for 100 h with a 0.5V potential hold revealed that while Fe-N-C catalysts have a high initial activity, they degrade rapidly within the first 24 h, beyond which their current density continued to decrease further. Whereas CN<sub>x</sub> catalysts had a lower initial activity, but showed significantly less degradation in the first 24 h, following which the current density reached a plateau and remained constant thereafter. Figure 7 shows the polarization curves obtained before and after the 100-hour hold. We are currently investigating compositional and structural differences between the two classes of catalysts via XPS, TEM, EXAFS, XANES, TPO techniques.

## Future Directions

In addition to investigating differences between CN<sub>x</sub> and Fe-N-C catalysts, we are examining the effect of acid washing on Fe-N-C catalysts, as well as the effect of duration of acid washing on the activity and stability of these catalysts.

We have also obtained preliminary results to show that CN<sub>x</sub> and Fe-N-C catalysts are active for ORR in alkaline medium, with activities comparable to platinum. This could have a direct implication on development of cathode catalysts for metal-air batteries or alkaline fuel cells. We will be developing button cells to test these materials as cathodes for zinc-air batteries.

## Publication list in the last year acknowledging the DOE grant or contract

1. Von Deak, D., Singh, D., Biddinger, E.J., King, J.C., Bayram, B., Miller, J.T., Ozkan, U.S., "Investigation of sulfur poisoning of CN<sub>x</sub> oxygen reduction catalysts for PEM fuel cells," *Journal of Catalysis*. **2012**, 285, 145-151.
2. Von Deak, D. Singh, D., King, J.C., Ozkan, U.S., "Von Deak, D. Singh, D., King, J.C., Ozkan, U.S., "Use of carbon monoxide and cyanide to probe the active sites on nitrogen-doped carbon catalysts for oxygen reduction," *Applied Catalysis, B.*, **2012**, 113-114, 126-133.
3. Ozkan, U.S., "Bridging Heterogeneous Catalysis and Electrocatalysis: Catalytic Reactions Involving Oxygen," accepted for publication in *Topics in Catalysis*
4. Singh, D., Soykal, I.I., von Deak, D., Tian, J., King, J., Miller, J.T., Ozkan, U.S., "Operando and *in-situ* characterization of the growth of CN<sub>x</sub> carbon nano-structures as oxygen reduction reaction catalysts," accepted to *Journal of Catalysis*.
5. Bao, X., Nie, X., von Deak, D., Biddinger, E.J., Luo, W., Asthagiri, A., Ozkan, U.S., Hadad, C.M., "A first-principles study of the role of quaternary-N doping on the oxygen reduction reaction activity and selectivity of graphene edge sites," accepted to *Topics in Catalysis*.